

PARP Inhibitor Activity Correlates with *SLFN11* Expression and Demonstrates Synergy with Temozolomide in Small Cell Lung Cancer**Authors:**

Benjamin H. Lok^{1,2}, Eric E. Gardner^{2,3}, Valentina E. Schneeberger², Andy Ni⁴, Patrice Desmeules⁵, Natasha Rekhtman⁵, Elisa de Stanchina⁶, Beverly A. Teicher⁷, Nadeem Riaz¹, Simon N. Powell^{1,8,9}, John T. Poirier^{2,9,10*}, Charles M. Rudin^{2,9,10*}

Affiliations:

¹Department of Radiation Oncology, Memorial Sloan Kettering Cancer Center, New York ,NY

²Molecular Pharmacology Program, Memorial Sloan Kettering Cancer Center, New York, NY

³Pharmacology Graduate Training Program, Department of Pharmacology and Molecular Sciences, Johns Hopkins University, Baltimore, MD

⁴Department of Epidemiology and Biostatistics, Memorial Sloan Kettering Cancer Center, New York, NY

⁵Department of Pathology, Memorial Sloan Kettering Cancer Center, New York, NY

⁶Anti-Tumor Assessment Core Facility, Memorial Sloan Kettering Cancer Center, New York, NY

⁷Division of Cancer Treatment and Diagnosis, National Cancer Institute, Bethesda, MD

⁸Molecular Biology Program, Memorial Sloan Kettering Cancer Center, New York, NY

⁹Weill Cornell Medical College, New York, NY

¹⁰Department of Medicine, Memorial Sloan Kettering Cancer Center, New York, NY

Running Title: SLFN11 Predicts PARP Inhibitor Response in SCLC

Keywords: PARP inhibition, small cell lung cancer, patient-derived xenografts, SLFN11, biomarker

Financial Support: This work was supported by BioMarin Pharmaceutical Inc., the National Cancer Institute (P30 CA008748, U54 OD020355-01, and R01 CA197936), Van Andel Research Institute, LUNGevity, and Free to Breathe, Conquer Cancer Foundation of ASCO, and Radiological Society of North America (RR1634).

***Co-corresponding Authors:**

Charles M. Rudin, MD, PhD (rudinc@mskcc.org)

Hassenfeld Professor and Chief, Thoracic Oncology Service, Memorial Sloan Kettering Cancer Center
Professor of Medicine, Weill Cornell Medical College

John T. Poirier, PhD (poirierj@mskcc.org)

Assistant Attending, Memorial Sloan Kettering Cancer Center
Assistant Professor of Medicine, Weill Cornell Medical College

Conflict of Interest: The authors have no conflicts of interest to disclose.

Word Count (excluding references): 5,139 words

Total Number of Figures and Tables: 6 Figures

Translational relevance (current: 145 words; max: 150 words)

There is a dire need for novel biomarker-directed therapeutics for small cell lung cancer (SCLC). In initial phase I studies, the PARP inhibitor talazoparib has shown clinical activity in some patients with SCLC, but predictive biomarkers of PARP inhibitor activity have not been defined. We investigated response predictors to PARP inhibitors (PARPi) and found *SLFN11*, but not scoring algorithms for homologous recombination deficiency, correlated with response. We demonstrated *SLFN11* correlates with PARPi sensitivity and is directly operant, through CRISPR-Cas9 and shRNA approaches. We confirmed in patient-derived xenografts that *SLFN11* assessment by immunohistochemical staining, a clinically applicable assay, predicted talazoparib response. Furthermore, we demonstrated temozolomide – recently added to the NCCN guidelines for SCLC 2nd line therapy – is strongly synergistic with PARPi *in vitro* and demonstrates combinatorial efficacy *in vivo*. These data support future biomarker-directed clinical investigation of PARPi in SCLC along with combinatorial therapy with temozolomide.

Abstract (current: 249 words; max: 250 words)

Purpose: PARP inhibitors (PARPi) are a novel class of small molecule therapeutics for small cell lung cancer (SCLC). Identification of predictors of response would advance our understanding, and guide clinical application, of this therapeutic strategy.

Experimental Design: Efficacy of PARP inhibitors olaparib, rucaparib, and veliparib, as well as etoposide and cisplatin in SCLC cell lines, and gene expression correlates, were analyzed using public datasets. HRD genomic scar scores were calculated from Affymetrix SNP 6.0 arrays. *In vitro* talazoparib efficacy was measured by cell viability assays. For functional studies, CRISPR-Cas9 and shRNA were used for genomic editing and transcript knockdown, respectively. Protein levels were assessed by immunoblotting and immunohistochemistry (IHC). Quantitative synergy of talazoparib and temozolomide were determined *in vitro*. *In vivo* efficacy of talazoparib, temozolomide, and the combination was assessed in patient-derived xenograft (PDX) models.

Results: We identified *SLFN11*, but not HRD genomic scars, as a consistent correlate of response to all three PARPi assessed, with loss of *SLFN11* conferring resistance to PARPi. We confirmed these findings *in vivo* across multiple PDX and defined IHC staining for *SLFN11* as a predictor of talazoparib response. As temozolomide has activity in SCLC, we investigated combination therapy with talazoparib and found marked synergy *in vitro* and efficacy *in vivo*, which did not solely depend on *SLFN11* or *MGMT* status.

Conclusions: *SLFN11* is a relevant predictive biomarker of sensitivity to PARP inhibitor monotherapy in SCLC and we identify combinatorial therapy with TMZ as a particularly promising therapeutic strategy that warrants further clinical investigation.

Introduction

Lung cancer is the most common cause of cancer death in both men and women, responsible for more deaths than colon cancer, breast cancer and prostate cancer combined. Small cell lung cancer (SCLC) represents approximately 15% of all lung cancers. SCLC is strongly associated with tobacco exposure, and is expected to be an increasingly prevalent concern over the next several decades, particularly in Asia and the developing world, mirroring smoking trends. Worldwide, more than 200,000 people die from SCLC every year. Overall 5-year survival for patients with SCLC is a dismal 7%, with almost all survivors being among the minority diagnosed with limited stage disease.

All standard therapies for SCLC are DNA damaging agents, inducing either covalent DNA adducts and crosslinks (cisplatin, carboplatin, temozolomide [TMZ]), or single-strand or double-strand breaks (ionizing radiation, etoposide, topotecan, irinotecan)(1-3). Despite its grim survival statistics, SCLC is also notable for being remarkably responsive to combinations of these DNA damaging agents. In fact, about 25% of patients with limited stage disease are cured with concomitant cisplatin, etoposide and radiation. The exceptional sensitivity to DNA-damaging therapies may relate to the underlying genetics driving SCLC oncogenesis. Nearly 100% of cases of SCLC have homozygous loss or inactivation of both *RB1*, encoding the primary regulator of the G1-S cell cycle checkpoint, and *TP53*, critical for multiple DNA damage response pathways(4). The notable sensitivity of SCLC to DNA damage suggests that targeted inhibition of the DNA repair pathways operant in SCLC is a particularly attractive strategy, and can substantially augment the efficacy of therapies in our current armamentarium.

Poly-(ADP)-ribose polymerase enzymes (PARP) function to detect and mark DNA single-strand breaks (SSB) by binding to the site of DNA damage and synthesizing poly-(ADP)-ribose chains, which recruit a host of scaffold proteins and DNA repair enzymes to resolve the break(5). PARP1 protein levels are upregulated in SCLC relative to other lung cancers, and initial studies suggested that this upregulation was associated with increased sensitivity of SCLC lines to PARP inhibitors *in vitro*(6). These promising preclinical data in SCLC supported the inclusion of a SCLC cohort in a phase I study of the PARP inhibitor talazoparib with promising initial signals of efficacy(7).

PARP1 was first described as a regulator of base excision repair, but has since been implicated in the function of homologous recombination (HR), non-homologous end joining and microhomology-mediated end joining(5, 8). There are at least two distinct mechanisms of action of PARP inhibitors:

enzymatic inhibition and the more recently recognized PARP trapping(9, 10). Inhibition of PARP enzymatic activity was initially thought to explain the synthetic lethality observed with PARP inhibitors in breast and ovarian cancers with *BRCA1/2* mutations. These mutations lead to deficiencies in HR, leaving these cancers highly dependent on PARP mediated repair(11, 12). The PARP inhibitor olaparib was recently approved for treatment of germline *BRCA1/2* mutant ovarian cancer patients based on the results of a randomized phase II study(13). In addition, the FDA granted olaparib Breakthrough Therapy designation for treatment of patients with castrate resistant metastatic prostate cancer harboring *BRCA1/2* and *ATM* mutations. However, mutations in *BRCA1/2* are notably rare ($\leq 3\%$) in SCLC based on recent comprehensive genomic analyses(4, 14).

PARP trapping is a distinct mechanism of action of PARP inhibitors, whereby the inhibitor/PARP complex becomes fixed on the DNA at sites of single-strand breaks, leading to a failure to repair, and, with replication, induction of multiple double strand breaks. PARP trapping may be responsible for synergy between PARP inhibitors and DNA damaging agents that increase the prevalence of single-strand breaks. Further, this mechanism may be operant in cancers without defined HR deficiencies(9). The various PARP inhibitors in clinical development and clinical use vary in relative potency for both enzymatic inhibition and PARP trapping effects. Olaparib and talazoparib have comparable levels of catalytic inhibition, while talazoparib is ~ 100 -fold more potent than olaparib at trapping PARP-DNA complexes(9, 10). Rucaparib appears to have activity similar to olaparib, while veliparib is less potent both in enzymatic inhibition and in trapping activity(9, 10).

Beyond inactivating mutations in known mediators of HR such as *BRCA1/2*, other mechanisms may result in HR deficiency in sporadic tumors, including epigenetic silencing of *BRCA1* and HR pathway disruptions in other known and unknown mediators of this pathway(15, 16). This has led to substantial interest in strategies for defining “BRCAness”, or HR deficiency (HRD), including using characteristic patterns of mutation and loss from whole exome sequencing data to generate HRD scores(17-19). Discovering novel mechanisms of HRD in sporadic tumors may broaden the therapeutic potential of PARP inhibitors.

In this study, we sought to define determinants of PARP inhibitor activity in SCLC, and also to evaluate the combinatorial activity of PARP inhibition with the DNA damaging agent TMZ. Recent studies have suggested that TMZ is a particularly effective agent in recurrent metastatic SCLC, with both systemic and central nervous system activity, leading to its inclusion in the National

Comprehensive Cancer Network guidelines for standard treatment of this disease(20). We report *Schlafen 11* (*SLFN11*) as a critical determinant of PARP inhibitor sensitivity in SCLC. *SLFN11* was recently reported to be actively recruited to sites of DNA damage, and to inhibit HR, strongly supporting these findings(21). We found the association between PARP trapping and cytotoxic activity is stronger in SCLC than in other tumor types, and focused subsequent analyses on the strongest PARP trapper, talazoparib. By CRISPR-Cas9 gene editing and shRNA approaches, we established that loss of *SLFN11* confers resistance to talazoparib in SCLC cell lines. *In vivo*, we confirmed *SLFN11* expression by immunohistochemistry (IHC) is associated with tumor response to talazoparib in multiple patient-derived xenograft (PDX) models. We also demonstrated marked synergy between talazoparib and TMZ in multiple SCLC cell lines, and that combinatorial treatment with talazoparib and TMZ extends the spectrum of activity beyond those tumors with high *SLFN11* levels. Collectively, our results demonstrate that *SLFN11* is a relevant predictive biomarker of sensitivity to PARP inhibitor monotherapy in SCLC, and support combinatorial therapy with TMZ as a promising therapeutic strategy in SCLC.

Materials and Methods

Cell lines and reagents

SCLC cell lines were purchased from American Type Culture Collection and maintained as recommended. All cell lines tested negative for mycoplasma and were short tandem repeat verified/authenticated within 6 months of use. Dimethyl sulfoxide (DMSO) was used as a vehicle for all *in vitro* experiments. Talazoparib was obtained from Biomarin or Selleck Chemicals. For *in vivo* use, talazoparib was prepared in dimethylacetamide (DMAc; 270555, Sigma) in 1 mg/mL concentration then diluted 1:10 in 5 parts Kolliphor HS/85 parts PBS and stored at 4°C and discarded after 14 days. For *in vivo* dosing, talazoparib was diluted in sterile PBS to 0.2mg/mL for weight-based dosing by oral gavage. Talazoparib vehicle was 2% DMAc/1% Kolliphor HS/ 97% PBS. Temozolomide (S1237; Selleck Chemicals) for *in vivo* use was prepared in 0.5% carboxymethylcellulose sodium salt in water for weight-based dosing by oral gavage.

Cell viability assays

Talazoparib and LT674 sensitivity

Cells were collected and suspended by exposure to Accutase in 300 ml of media, then plated (5x10³ - 20x10³ in 42 ul) in 384-well plates (CulturPlates, PE, Waltham, MA) 24 hours prior to treatment. Each compound was tested at 9 different concentrations (10 uM to 1.5 nM; DMSO concentration 0.25%), then the plates were incubated for 96 hrs. The incubation was terminated by adding ATP Lite (Perkin Elmer Inc., Waltham, MA) and luminescence was determined.

CRISPR/Cas9 and custom shRNA cell lines

Cells were plated 24 hours before treatments in 96-well plates at 1x10³ – 5x10³ cells per well. Viability (AlamarBlue; ThermoFisher) assays were quantified on a compatible plate reader. Cell lines were treated with the indicated drugs for 5 to 7 days prior to assaying.

Antibodies and Western blots

Primary antibodies to SLFN11 (Santa Cruz; sc-374339), PARP1 (Santa Cruz; sc-7150) and used at a 1:250 and 1:1000 dilution, respectively, according to manufacturer's instructions. Primary antibodies to MGMT (Cell Signaling Technology; #2739) and actin (Cell Signaling Technology; #4967) were used at a 1:1000 dilution.

For quantitative infrared Western blots, all products and reagents unless specified were purchased from LI-COR Biosciences and used according to the manufacturer's recommendations (see Supplemental Methods). For film developed Western blots, enhanced chemiluminescence (ECL) detection anti-mouse or anti-rabbit HRP-conjugated secondary antibodies (GE Healthcare) were used at a 1:5000 dilution as previously described(22). Target protein quantification was normalized relative to the highest loading control sample.

Immunohistochemistry (IHC)

The IHC detection of *SLFN11* antibody (Sigma-Aldrich; HPA023030) was performed at the Molecular Cytology Core Facility of Memorial Sloan Kettering Cancer Center using Discovery XT processor (Ventana Medical Systems,Tucson AZ). *SLFN11* primary incubation time is 5 hours, followed by 60 min incubation with biotinylated goat anti-rabbit IgG (Vector, cat # BA-1000, 1:200 dilution), Blocker D, Streptavidin- HRP and DAB detection kit (Ventana Medical Systems) were used according to the manufacturer instructions.

Establishment of *SLFN11* cell lines

*Custom shRNA approach against *SLFN11**

Custom shRNA miR-E sequences designed to target *SLFN11* were as follows:

SLFN11#1:

TGCTGTTGACAGTGAGCGCTAGAAGTAATCCTTCATTAAATAGTGAAGCCACAGATGTATTAAATGAAGG
ATTACTTCTAACGCCTACTGCCCTCGGA;

SLFN11#2:

TGCTGTTGACAGTGAGCGATCAGACCAATATCCAAGAGAATAGTGAAGCCACAGATGTATTCTCTGGAT
ATTGGTCTGAGTGCCTACTGCCCTCGGA.

A control shRNA targeting Renilla Luciferase has been previous described(23). These constructs were generated and cloned into the LT3GEPIR (pRRL) vector, which was a gift from Christof Fellmann and Johannes Zuber, then transfected into the cell lines of interest.

SLFN11 knockout by CRISPR-Cas9

The lentiCRISPR v2 plasmid was a gift from Feng Zhang (Addgene plasmid #52961). The design of sgRNAs targeting *SLFN11* was performed using publically available software. Guide pairs were synthesized by Sigma Aldrich, annealed and inserted into the lentiCRISPR v2 backbone as described previously (24). sgRNA sequences and plasmids were confirmed by Sanger sequencing and are as

follows: SLFN11#1, 1F: AGGTATTCCTGAAGCCGAA, 1R: TTCGGCTTCAGGAAATACCTC; SLFN11#2, 2F: GAGTCCTGAGAGCAGCGCAG, 2R: CTGCGCTGCTCTCAGGACTCC.

Lentiviral transfections/ Lentiviral transductions

See Supplemental Methods.

Homologous recombination deficiency genomic scar assay

Affymetrix SNP6 array data from the CCLE were processed together, quantile-normalized, and median-polished with Affymetrix power tools(25). The birdseed algorithm was used for genotyping. PennCNV was employed to generate log R ratio and B-allele frequencies(26). ASCAT was used to generate allele-specific copy number information, which was then used to compute LST, N_{tAI}, HRD-LOH scores in the R statistical environment (v3.0.2) following methods outlined in the initial publications(17-19).

Gene expression analysis in cancer cell lines

Robust Multi-array Average (RMA) and quantile normalized gene expression microarray data for 1,037 cancer cell lines was downloaded from the Cancer Cell Line Encyclopedia(25).

Gene expression analysis in primary human tumors

Publically available gene expression datasets from The Cancer Genome Atlas were combined with our previously published genomic dataset of primary human SCLC tumors(14). The results published here are in part based upon data generated by the TCGA Research Network.

SCLC PDX models and dosing

The PDXs were isolated and passaged as previously described (27, 28). All treatment and toxicity experiments were performed in female NSG mice (NOD.Cg-*Prkdc*^{scid} *Il2rg*^{tm1Wjl}/SzJ; The Jackson Laboratory) that were 6 to 8 weeks old at time of PDX injection/implantation.

Tumor volumes were calculated from manual caliper measurements with an ellipsoid formula in which volume (mm³) = (xy²)/2. Once tumor volumes reached approximately 150mm³, mice were randomized to treatment arms and treated via oral gavage with vehicles, talazoparib (0.2 mg/kg or 0.3 mg/kg) daily, TMZ (6 mg/kg) every 4 days, or in combination (talazoparib 0.2mg/kg daily and TMZ 6 mg/kg every 4 days).

Statistics

Gene expression analysis was performed using the R statistical programming environment and the Bioconductor suite of tools. Expression values for 23 SCLC samples were centered and 12,631 genes with mean absolute deviation >.3 were considered. Genes with expression correlating with mean PARP inhibitor response *in vitro* were identified using LIMMA to fit a linear model to each gene and generate moderated *t*-statistics using an empirical Bayes approach, including as covariates *PARP1* gene expression, and LST score. *p*-values were adjusted for multiple testing by the method of Benjamini and Hochberg. Spearman's rank correlation performed on drug response data and HRD scores to talazoparib response.

All animal data are reported as average tumor volumes ± SD. Tumor volume comparisons between treatment groups used data from study end point using a two-sided Student *t* test; throughout the text unless indicated: *, *p* < 0.05 and **, *p* < 0.01. All graphs in figures were created using GraphPad Prism 6.0c (GraphPad Software, Inc.) or R (version 3.2.2).

Linear mixed effect models were fit on individual animal data to assess whether response to talazoparib depends on SLFN11 expression, which was represented by the interaction between talazoparib treatment and SLFN11 expression. We used various measurements to represent SLFN11 expression in the model including IHC staining H-score, modified H-score, dichotomized H-score, Western blot, and mRNA level. The outcome was the end point tumor volume. The start tumor volume was included in the regression model as a covariate. Random intercepts were used to account for the clustering of animals within PDX models.

Assessment of drug synergy

Drug synergy was determined quantitatively using the combination index (CI) method of Chou and Talalay(29). Viability was calculated across a wide range of doses for talazoparib and temozolomide individually and in combination as a constant ratio of talazoparib to temozolomide (1:10,000 and 1:2,500). CI was calculated as a function of response or fraction affected (Fa) using the formula $CI = (D_1)/(D_x)_1 + (D_2)/(D_x)_2$ where D_1 and D_2 are the doses used to achieve a specific response in combination and $(D_x)_1$ and $(D_x)_2$ are individual drug doses needed to achieve similar response with CompuSyn Software ver. 2005. A $CI > 1$ indicates antagonism, while a $CI < 1$ indicates synergism.

Study Approval

All animal experiments were performed in accordance with protocols approved by the Institutional Animal Care and Use Committee of Memorial Sloan Kettering Cancer Center.

Results

DNA damaging agents exhibit a range of drug sensitivity in SCLC cell lines that is not predicted by HRD genomic scars or PARP1 expression

We initially sought to determine whether previously defined assays for HRD could predict SCLC sensitivity to PARP inhibitors. The activity of cisplatin, like that of PARP inhibitors, has been previously reported to correlate with HRD scores in patients with breast and ovarian cancers(17-19). For analysis in SCLC, we evaluated the relative activity of olaparib, racuparib, and veliparib across 414 cell lines available from the Genomics of Drug Sensitivity in Cancer (GDSC) panel, including 23 SCLC cell lines(30). The observed responses to all 3 agents were correlated across all histologies, including SCLC (Fig 1A).

Large chromosomal structural alterations characteristic of *BRCA1/2* mutant cancers have been deployed as an indirect assessment of HRD, representing a history of “scarring” of the genome reflective of loss of this particular repair pathway. Three metrics of these HRD genomic scars are: loss of heterozygosity (HRD-LOH), large-scale state transition (LST), and telomeric allelic imbalance (N_{tAI})(17-19, 31). These HRD measures correlate with platinum sensitivity in sporadic triple-negative breast and ovarian cancers(17-19, 32, 33). We hypothesized that HRD scores might be a relevant response discriminator to PARP inhibitors in SCLC. To interrogate this premise, we computed the three different HRD metrics (HRD-LOH, LST, N_{tAI}) in SCLC cell lines using publicly available Cancer Cell Line Encyclopedia (CCLE) Affymetrix SNP 6.0 array datasets (Supplemental Fig 1 and Supplemental Table 1)(17-19, 25). Across this dataset, all three measures correlated with one another, but surprisingly, none of these three measures of HRD correlated with response to PARP inhibitor sensitivity *in vitro* in SCLC (Supplemental Fig 1B). Consistent with previous work(6), we found PARP1 is overexpressed in SCLC by gene transcript levels (*data not shown*). We then quantified PARP1 protein levels by near infrared Western blotting (Supplemental Fig 2A). Unsurprisingly, as PARP1 protein levels are almost universally high in SCLC cell lines relative to NSCLC(6), expression of PARP1 itself was not informative for response to PARP inhibition in linear regression analysis (Supplemental Fig 2B).

SLFN11* expression predicts sensitivity to PARP inhibition *in vitro

We sought to identify other features that might better predict SCLC sensitivity to PARP inhibition. Using Robust Multi-array Average (RMA) data from the CCLE, we analyzed expression of 12,631 genes in 414 cell lines to identify candidate determinants of PARP inhibitor activity with potential

relevance in SCLC. *SLFN11* was among the top genes most significantly correlated with PARP inhibitor sensitivity, controlling for HRD score and expression of *PARP1* and *PARP2* (Fig 1B and Supplemental Table 2). We observed that SCLC cell lines with high levels of *SLFN11* transcript were more sensitive to PARP inhibitors and conventional cytotoxic therapy (Fig 1C). Interestingly, across the three PARP inhibitors studied, a lower differential in activity between SCLC and other cell lines was evident in drugs with more potent PARP trapping ability (i.e. olaparib > rucaparib > veliparib; Fig 1D).

Due to this correlation of PARP trapping potency and efficacy in SCLC, we conducted additional analyses with talazoparib, currently the most potent PARP trapper available in clinical development. Here, we tested a panel of SCLC cell lines and found, as previously reported, stereospecific drug activity (Fig 2A)(10). We confirmed that *SLFN11* transcript and protein expression correlate, by linear regression ($p = 0.01$; Supplemental Fig 2C). As expected, we established that *SLFN11* expression is a determinant of talazoparib sensitivity where a correlative trend by linear regression between *SLFN11* protein expression and talazoparib sensitivity was observed, even in this small sample ($p = 0.06$; Fig 2B).

Loss of *SLFN11* confers resistance to PARP inhibition in SCLC

These correlative analyses suggested that *SLFN11* might be a direct determinant of PARP inhibitor activity in SCLC. Alternatively, *SLFN11* expression could correlate with PARP inhibitor sensitivity reflecting a shared association with another determining factor. To test these alternative hypotheses, we directly assessed whether *SLFN11* inactivation conferred PARP inhibitor resistance by deriving SCLC cell lines with doxycycline inducible expression of 2 different shRNA sequences targeting *SLFN11*. We observed that knockdown resulted in a \geq log-fold increase in the talazoparib IC₅₀, supporting a direct role for *SLFN11* in drug sensitivity (Fig 3A, Supplemental Fig 3). To further confirm this result, we employed CRISPR-Cas9 gene editing to derive *SLFN11* knockout cells. We observed the same talazoparib resistance phenotype in the most effective guide RNA tested, when employing a pooled selection approach to generate knockout cell lines (*SLFN11*-KO#2; Fig 3B). The parental cell line and a different sgRNA sequence with inefficient knockout (*SLFN11*-KO#1) served as negative controls (Fig 3B).

In vivo* PARP inhibitor efficacy in SCLC PDXs requires *SLFN11

We have previously shown that SCLC PDX models more closely reflect their tumors of origin than standard cell line xenografts, which demonstrate gene expression alterations attributable to *ex vivo*

cell line derivation(28). Novel therapeutic testing in PDXs in several instances appears to more accurately reflect the subsequent experience in humans(27, 34-37). These observations have recently led the NCI to announce plans to retire the NCI-60 cell line panel and replace this with a PDX repository as the preferred platform for drug discovery and testing. Therefore, we conducted *in vivo* testing in our available PDX models.

We characterized 7 SCLC PDXs for *SLFN11* protein expression by IHC staining (Fig 4A) and conducted talazoparib efficacy experiments in each tumor model. We found talazoparib dosed daily at 0.3 mg/kg was well tolerated (Supplemental Fig 4A). Efficacy data *in vivo* was entirely consistent with the cell line observations that *SLFN11* expression was required for sensitivity to talazoparib. All 3 PDX models that were *SLFN11*-high demonstrated statistically significant and clinically meaningful tumor growth inhibition (TGI) with single agent talazoparib, whereas none of the 4 *SLFN11*-low models responded (Fig 4B and C). A thoracic pathologist blinded to PDX identity and response data generated a *SLFN11* H-score, which ranges from 0 - 300 and integrates three intensities of IHC nuclear staining and their frequency (Fig 4A). We used a linear mixed effect model to confirm the strong dependence of talazoparib efficacy on *SLFN11* expression ($p < 0.0001$ for the interaction). The difference in the end point tumor volume between talazoparib and control groups increases by 6.83mm³ for every unit increase in the *SLFN11* H-score (95% confidence interval: 4.25 to 9.41 mm³; Supplemental Fig 4C and Supplemental Table 3). Interestingly, *SLFN11* H-score proved to be a stronger predictor of talazoparib efficacy across these PDX lines than either *SLFN11* gene expression, or protein expression by Western blot (Statistical Model #1 vs. #4 and #5 in Supplemental Table 3 and Supplemental Fig 4B and C). We also found a modified H-score consisting of the grouped nuclear staining intensities 2+ and 3+ categories as a robust predictor of talazoparib response (Fig 4A, Supplemental Fig 4D, and Supplemental Table 3). These observations have practical ramifications: the ability to quantitatively assess *SLFN11* by IHC staining will facilitate rapid clinical translation, allowing evaluation of formalin-fixed paraffin embedded samples.

***SLFN11* has a range of expression in human primary SCLC tumors allowing for use as a biomarker**

We evaluated gene expression levels for *SLFN11* in treatment naïve SCLC patient tumors available from our previously published work(14) and retrieved datasets from other tumor histologies available as part of The Cancer Genome Atlas (TCGA). We found that *SLFN11* was highly expressed in SCLC as compared to other histologies (Fig 4D). In addition, we observed a bimodal distribution

of *SLFN11* gene expression (Fig 4D, *right inset, blue dashed line*), that may provide meaningful stratification as a predictive biomarker in future clinical studies of SCLC.

PARP inhibition is synergistic with TMZ independent of *MGMT* or *SLFN11* status

Clinical evaluations of PARP inhibitor efficacy are increasingly shifting to combination studies focusing, in particular, on co-administration with DNA damaging agents. Of particular interest, previous studies have demonstrated combinatorial efficacy between PARP inhibitors and TMZ across multiple disease types including colon cancer, breast cancer, melanoma, leukemia, and glioblastoma(38-42). As noted above, TMZ is of particular relevance in SCLC, as it possesses substantial activity in recurrent metastatic SCLC, including patients with brain metastases.

TMZ is a DNA alkylator that preferentially methylates the O6 position of guanine. *MGMT*, a demethylating DNA repair protein, reverses the O6 methylation caused by TMZ, and silencing of the *MGMT* gene by promoter hypermethylation has been correlated with improved tumor response and overall survival to TMZ in combination with radiotherapy in glioblastoma(43). Initial clinical data in SCLC also revealed a trend ($p = 0.08$) toward higher response to TMZ in patients with *MGMT* promoter silencing(20).

We therefore sought to evaluate the combinatorial activity of TMZ and talazoparib across our panel of SCLC models, and to assess the predictive roles of both *MGMT* expression and *SLFN11* expression in this context. We first performed a drug synergy matrix of 35 different combinations of talazoparib and TMZ dose levels (Fig 5A, *left*). We found a range of combinations between 1 : 70, and 1 : 700,000 of talazoparib to TMZ that exhibited excess response over highest single agent (HSA) activity and determined a 1 : 10,000 ratio of talazoparib : TMZ to be the approximate median drug ratio (Fig 5A, *right*).

We then performed formal assessments of combinatorial synergy of TMZ and talazoparib using 4 cell lines, 2 with high *MGMT* expression (H82, DMS114) and 2 with low *MGMT* expression (H446, H146; Fig 5B). We performed combination index (CI) experiments as described by Chou and Talalay(29) to quantify any synergistic interaction between talazoparib and TMZ. Cells were treated with talazoparib or TMZ alone, or a fixed ratio of 1 : 10,000 of talazoparib : TMZ (range tested 0.25 nM : 25 μ M to 16 nM : 160 μ M).

All 4 cell lines exhibited strong synergism, although in distinct dose ranges. Low combination doses (≥ 0.5 nM : 5 μ M) were sufficient for clear synergy in *MGMT* low lines (H446, H146). However, for

the MGMT high lines (H82 and DMS114) a 4-fold increase in combination doses (≥ 2 nM : 20 μ M) was necessary for synergism (Fig 5C and D; Supplemental Fig 5A). This difference may be attributable to a requirement of achieving TMZ concentrations that exceed the demethylating capacity of MGMT. We confirmed similar findings with a lower talazoparib to TMZ ratio of 1 : 2,500, that coincided with the greatest excess over HSA, where synergy was seen in combination doses with at least 10 μ M of TMZ (Supplemental Fig 5B and C).

Finally, we evaluated the combination of TMZ and talazoparib across the same 7 PDX models in which we had established data on talazoparib single agent activity. We hypothesized that this combination might extend the utility of PARP inhibition beyond the confines of *SLFN11*-high disease. We first determined a well tolerated combination regimen of talazoparib 0.2 mg/kg daily and TMZ 6 mg/kg q4d (Supplemental Fig 4A). We then conducted comparative assessment of each single agent versus the combination of TMZ and talazoparib across all 7 models (Fig 6A and Supplemental Fig 6). We found that the combination exhibited significantly greater TGI than either single agent in multiple PDX models, although the combinatorial efficacy was particularly striking in high *SLFN11*-expressing models (i.e. JHU-LX22, JHU-LX110, SCRX-Lu149; Fig 6A). Interestingly, in these models, MGMT expression levels did not appear to correlate with single agent TMZ or combinatorial response (Fig 6A and B). Notably, one MGMT low PDX, JHU-LX48, exhibited dramatic sensitivity to TMZ, with marked tumor regression in all treated animals and with 2 of 5 animals in the TMZ treatment group and 3 of 5 animals in the combination treatment group having no tumor regrowth up to 180 days after the last TMZ dose was given. Other factors beyond the lack of MGMT expression are likely to contribute to TMZ efficacy in this exceptional responder. Collectively, these combinatorial treatment response data suggest that talazoparib and TMZ appear to be a highly promising combination therapy for SCLC.

Discussion

PARP inhibition is a novel and promising therapy in SCLC, a recalcitrant disease where therapeutic advances have been limited. To date, the only response predictors associated with PARP inhibitor activity in cancer have been *BRCA1/2* and *ATM* mutations in breast, ovarian and prostate cancers. No such predictive biomarker has been defined for SCLC. Previous *in vitro* analyses in colon cancer and Ewing sarcoma cell lines have implicated *SLFN11* as a correlate of response to conventional DNA damaging agents, including topoisomerase poisons and cisplatin (25, 44, 45). In this study, we substantially expand our knowledge of *SLFN11* by showing for the first time that *SLFN11* is a strong predictor of SCLC sensitivity to PARP inhibitors, and confirm these findings *in vivo* through multiple PDX models. In addition, we show that IHC staining against *SLFN11* is a particularly strong predictor of PARP inhibitor response in PDXs, a finding that has immediate clinical translational implications. Finally, we show that combination therapy of a PARP inhibitor with TMZ is synergistic, well-tolerated and effective across multiple SCLC cell lines and PDXs.

Mu and colleagues recently presented an analysis of *SLFN11* protein mechanisms of action, demonstrating direct interaction with replication protein A (RPA) 1, destabilization of RPA-ssDNA complexes, and ultimately inhibition of HR as observed in sister chromatid exchange and I-SceI fluorescent reporter gene conversion assays(21). These important data provide an evident mechanism for our series of observations indicating that *SLFN11* confers PARP inhibitor sensitivity in SCLC. Together these studies suggest that high *SLFN11* expression is a novel and potent mechanism of establishing a BRCA-like state of HRD, not necessarily reflected in current HRD scoring metrics, that governs sensitivity to PARP inhibitors and may dictate sensitivity to DNA damaging agents more generally.

We were surprised to find that all three HRD assays based on analysis of preexisting genomic scars failed to correlate with SCLC sensitivity to PARP inhibition. Our data suggest that *SLFN11* upregulation could represent a more dynamic mechanism of HRD than germline BRCA gene deficiency, and predicts PARP inhibitor sensitivity in SCLC without being evident in the analyses of genomic scarring which may take many cell generations to accumulate. At least in SCLC, *SLFN11* appears to be a more predictive biomarker of PARP inhibitor efficacy than HRD assays, which may in part reflect the high false positive rates of HRD scoring algorithms (31). Functional HR assays, for example *ex vivo* IHC evaluation of RAD51 nuclear localization after DNA damage, may provide a method to integrate these findings, circumventing the low positive predictive value of the HRD genomic scar assays and allowing for further refinement of these molecular biomarkers in

prospective clinical trials(16, 22, 46). Of note, alternatively, it is possible that *SLFN11* confers a distinct pattern of genomic instability that is not detected by these aforementioned HRD scar assays and is worthy of future investigation.

The potential for dynamic regulation of *SLFN11* expression suggests epigenetic modification as a potential therapeutic strategy. It has been shown that *SLFN11* promoter hypermethylation correlates with resistance to platinum agents and that DNA methyltransferase (DNMT) chemical inhibition or genetic loss reverses the hypermethylated state, thereby resensitizing cells to platinum drugs through *SLFN11* re-expression *in vitro*(47). As DNMT inhibitors are currently FDA approved for hematologic diseases, utilization of these epigenetic modifying drugs in overcoming *SLFN11* promoter methylation-dependent resistance to DNA damaging agents represents an attractive avenue to explore in future studies.

One interesting finding from our study is the observation that relative PARP inhibitor sensitivity in SCLC correlated more strongly with trapping potency than was observed in any other tumor type. Our results suggest that in the context of SCLC, PARP trapping may be the governing mechanism of drug efficacy. We eagerly await the results of the early SCLC clinical trials with talazoparib, the most potent PARP trapper available, as well as potential studies with other PARP inhibitors to provide evidence for or against this preclinical observation. Our expectations for such studies are tempered by our emerging data suggesting *SLFN11* suppression contributes to acquired resistance to cytotoxic chemotherapy in SCLC(48). These data suggest that recurrent/relapsed SCLC patients may exhibit lower expression levels of *SLFN11*, and imply that clinical trials examining PARP inhibitors as monotherapy in the second- or later-line settings may demonstrate suboptimal efficacy due to resistance conferred by loss of *SLFN11*. Notably, the broader activity in combination with TMZ may allow for greater benefit in the context of recurrent disease.

As combination therapies can increase disease control and may inhibit development of drug resistance, we explored the combination of talazoparib with TMZ, one of the few second-line agents for SCLC recognized in the National Comprehensive Cancer Network guidelines. We demonstrated in SCLC cell lines and PDX drug efficacy experiments PARP inhibitors synergize with TMZ *in vitro* and demonstrate strong combinatorial efficacy *in vivo*. These results are in line with encouraging results in other histologies(39-41, 49, 50). These promising results warrant future clinical investigation, and such trials are currently being planned. Future prospective clinical trials will ultimately be needed to validate these promising preclinical findings.

In conclusion, we demonstrate that the role of *SLFN11*-dependent drug sensitivity extends beyond conventional DNA damaging agents to a targeted agent, is operant in SCLC, and combination therapy of PARP inhibitors with TMZ is a opportune therapeutic strategy. Future work in our laboratory will focus on investigating strategies to manipulate *SLFN11* expression in tumors to increase the therapeutic ratio of PARP inhibition and other DNA damaging agents. Additional work will be necessary to translate these promising findings into biomarker-informed clinical trials of PARP inhibitors in SCLC.

Author Contributions

BHL, JTP, and CMR designed and conceived the study.

BHL, EEG, VES, and BAT designed and performed experiments.

BHL, AN, N. Riaz, and JTP performed biostatistical analyses.

PD performed histological/pathological analyses.

BHL, JTP , and CMR wrote the manuscript.

All authors edited the manuscript.

N. Rekhtman, ED, SNP, JTP and CMR supervised the study.

Acknowledgements

The authors thank Xiaodong Huang and the members of the Anti-Tumor Assessment Core Facility for their technical assistance; Afsar Barlas and Katia O. Manova-Todorova of the Molecular Cytology Core Facility for assistance with immunohistochemical staining; Hsiu-Yu Liu and Ralph J. Garippa of the RNAi Core Facility for assistance with custom shRNA constructs; Y. Jerry Shen and G. Karen Yu of Biomarin Pharmaceutical Inc. and all members of the Rudin laboratory for their helpful discussions. This study was supported by BioMarin Pharmaceutical Inc., the National Cancer Institute P30 CA008748, U54 OD020355-01, and R01 CA197936 (CMR), LUNGevity, Free to Breathe (JTP), Conquer Cancer Foundation of ASCO, and Radiological Society of North America RR1634 (BHL). Additional research funding provided by Van Andel Research Institute through the Van Andel Research Institute – Stand Up To Cancer Epigenetics Dream Team. Stand Up To Cancer is a program of the Entertainment Industry Foundation, administered by AACR.

References

1. Pietanza MC, Byers LA, Minna JD, Rudin CM. Small cell lung cancer: will recent progress lead to improved outcomes? *Clin Cancer Res.* 2015;21:2244-55.
2. Turrisi AT, 3rd, Glover DJ, Mason BA. A preliminary report: concurrent twice-daily radiotherapy plus platinum-etoposide chemotherapy for limited small cell lung cancer. *Int J Radiat Oncol Biol Phys.* 1988;15:183-7.
3. O'Brien ME, Ciuleanu TE, Tsekov H, Shparyk Y, Cucevia B, Juhasz G, et al. Phase III trial comparing supportive care alone with supportive care with oral topotecan in patients with relapsed small-cell lung cancer. *J Clin Oncol.* 2006;24:5441-7.
4. George J, Lim JS, Jang SJ, Cun Y, Ozretic L, Kong G, et al. Comprehensive genomic profiles of small cell lung cancer. *Nature.* 2015;524:47-53.
5. Rouleau M, Patel A, Hendzel MJ, Kaufmann SH, Poirier GG. PARP inhibition: PARP1 and beyond. *Nat Rev Cancer.* 2010;10:293-301.
6. Byers LA, Wang J, Nilsson MB, Fujimoto J, Saintigny P, Yordy J, et al. Proteomic profiling identifies dysregulated pathways in small cell lung cancer and novel therapeutic targets including PARP1. *Cancer Discov.* 2012;2:798-811.
7. Wainberg ZA, Rafii S, Ramanathan RK, Mina LA, Byers LA, Chugh R, et al. Safety and antitumor activity of the PARP inhibitor BMN673 in a phase 1 trial recruiting metastatic small-cell lung cancer (SCLC) and germline BRCA-mutation carrier cancer patients. *J Clin Oncol.* 2014;32:(suppl; abstr 7522).
8. El-Khamisy SF, Masutani M, Suzuki H, Caldecott KW. A requirement for PARP-1 for the assembly or stability of XRCC1 nuclear foci at sites of oxidative DNA damage. *Nucleic Acids Res.* 2003;31:5526-33.
9. Murai J, Huang SY, Das BB, Renaud A, Zhang Y, Doroshow JH, et al. Trapping of PARP1 and PARP2 by Clinical PARP Inhibitors. *Cancer Res.* 2012;72:5588-99.
10. Murai J, Huang SY, Renaud A, Zhang Y, Ji J, Takeda S, et al. Stereospecific PARP trapping by BMN 673 and comparison with olaparib and rucaparib. *Mol Cancer Ther.* 2014;13:433-43.
11. Farmer H, McCabe N, Lord CJ, Tutt AN, Johnson DA, Richardson TB, et al. Targeting the DNA repair defect in BRCA mutant cells as a therapeutic strategy. *Nature.* 2005;434:917-21.
12. Fong PC, Boss DS, Yap TA, Tutt A, Wu P, Mergui-Roelvink M, et al. Inhibition of poly(ADP-ribose) polymerase in tumors from BRCA mutation carriers. *N Engl J Med.* 2009;361:123-34.
13. Kaufman B, Shapira-Frommer R, Schmutzler RK, Audeh MW, Friedlander M, Balmana J, et al. Olaparib monotherapy in patients with advanced cancer and a germline BRCA1/2 mutation. *J Clin Oncol.* 2015;33:244-50.
14. Rudin CM, Durinck S, Stawiski EW, Poirier JT, Modrusan Z, Shames DS, et al. Comprehensive genomic analysis identifies SOX2 as a frequently amplified gene in small-cell lung cancer. *Nat Genet.* 2012;44:1111-6.
15. Esteller M, Silva JM, Dominguez G, Bonilla F, Matias-Guiu X, Lerma E, et al. Promoter hypermethylation and BRCA1 inactivation in sporadic breast and ovarian tumors. *J Natl Cancer Inst.* 2000;92:564-9.
16. Lord CJ, Ashworth A. BRCAness revisited. *Nat Rev Cancer.* 2016;16:110-20.
17. Abkevich V, Timms KM, Hennessy BT, Potter J, Carey MS, Meyer LA, et al. Patterns of genomic loss of heterozygosity predict homologous recombination repair defects in epithelial ovarian cancer. *Br J Cancer.* 2012;107:1776-82.
18. Birkbak NJ, Wang ZC, Kim JY, Eklund AC, Li Q, Tian R, et al. Telomeric allelic imbalance indicates defective DNA repair and sensitivity to DNA-damaging agents. *Cancer Discov.* 2012;2:366-75.

19. Popova T, Manie E, Rieunier G, Caux-Moncoutier V, Tirapo C, Dubois T, et al. Ploidy and large-scale genomic instability consistently identify basal-like breast carcinomas with BRCA1/2 inactivation. *Cancer Res.* 2012;72:5454-62.
20. Pietanza MC, Kadota K, Huberman K, Sima CS, Fiore JJ, Sumner DK, et al. Phase II trial of temozolomide in patients with relapsed sensitive or refractory small cell lung cancer, with assessment of methylguanine-DNA methyltransferase as a potential biomarker. *Clin Cancer Res.* 2012;18:1138-45.
21. Mu Y, Lou J, Srivastava M, Zhao B, Feng XH, Liu T, et al. SLFN11 inhibits checkpoint maintenance and homologous recombination repair. *EMBO Rep.* 2016;17:94-109.
22. Lok BH, Carley AC, Tchang B, Powell SN. RAD52 inactivation is synthetically lethal with deficiencies in BRCA1 and PALB2 in addition to BRCA2 through RAD51-mediated homologous recombination. *Oncogene.* 2013;32:3552-8.
23. Fellmann C, Hoffmann T, Sridhar V, Hopfgartner B, Muhar M, Roth M, et al. An optimized microRNA backbone for effective single-copy RNAi. *Cell Rep.* 2013;5:1704-13.
24. Shalem O, Sanjana NE, Hartenian E, Shi X, Scott DA, Mikkelsen TS, et al. Genome-scale CRISPR-Cas9 knockout screening in human cells. *Science.* 2014;343:84-7.
25. Barretina J, Caponigro G, Stransky N, Venkatesan K, Margolin AA, Kim S, et al. The Cancer Cell Line Encyclopedia enables predictive modelling of anticancer drug sensitivity. *Nature.* 2012;483:603-7.
26. Wang K, Li M, Hadley D, Liu R, Glessner J, Grant SF, et al. PennCNV: an integrated hidden Markov model designed for high-resolution copy number variation detection in whole-genome SNP genotyping data. *Genome Res.* 2007;17:1665-74.
27. Hann CL, Daniel VC, Sugar EA, Dobromilskaya I, Murphy SC, Cope L, et al. Therapeutic efficacy of ABT-737, a selective inhibitor of BCL-2, in small cell lung cancer. *Cancer Res.* 2008;68:2321-8.
28. Daniel VC, Marchionni L, Hierman JS, Rhodes JT, Devereux WL, Rudin CM, et al. A primary xenograft model of small-cell lung cancer reveals irreversible changes in gene expression imposed by culture in vitro. *Cancer Res.* 2009;69:3364-73.
29. Chou TC, Talalay P. Quantitative analysis of dose-effect relationships: the combined effects of multiple drugs or enzyme inhibitors. *Adv Enzyme Regul.* 1984;22:27-55.
30. Garnett MJ, Edelman EJ, Heidorn SJ, Greenman CD, Dastur A, Lau KW, et al. Systematic identification of genomic markers of drug sensitivity in cancer cells. *Nature.* 2012;483:570-5.
31. Watkins JA, Irshad S, Grigoriadis A, Tutt AN. Genomic scars as biomarkers of homologous recombination deficiency and drug response in breast and ovarian cancers. *Breast Cancer Res.* 2014;16:211.
32. Telli ML, Jensen KC, Vinayak S, Kurian AW, Lipson JA, Flaherty PJ, et al. Phase II Study of Gemcitabine, Carboplatin, and Iniparib As Neoadjuvant Therapy for Triple-Negative and BRCA1/2 Mutation-Associated Breast Cancer With Assessment of a Tumor-Based Measure of Genomic Instability: PrECOG 0105. *J Clin Oncol.* 2015;33:1895-901.
33. Isakoff SJ, Mayer EL, He L, Traina TA, Carey LA, Krag KJ, et al. TBCRC009: A Multicenter Phase II Clinical Trial of Platinum Monotherapy With Biomarker Assessment in Metastatic Triple-Negative Breast Cancer. *J Clin Oncol.* 2015;33:1902-9.
34. Gandhi L, Camidge DR, Ribeiro de Oliveira M, Bonomi P, Gandara D, Khaira D, et al. Phase I study of Navitoclax (ABT-263), a novel Bcl-2 family inhibitor, in patients with small-cell lung cancer and other solid tumors. *J Clin Oncol.* 2011;29:909-16.
35. Rudin CM, Hann CL, Garon EB, Ribeiro de Oliveira M, Bonomi PD, Camidge DR, et al. Phase II study of single-agent navitoclax (ABT-263) and biomarker correlates in patients with relapsed small cell lung cancer. *Clin Cancer Res.* 2012;18:3163-9.
36. Oltersdorf T, Elmore SW, Shoemaker AR, Armstrong RC, Augeri DJ, Belli BA, et al. An inhibitor of Bcl-2 family proteins induces regression of solid tumours. *Nature.* 2005;435:677-81.

37. Poirier JT, Gardner EE, Connis N, Moreira AL, de Stanchina E, Hann CL, et al. DNA methylation in small cell lung cancer defines distinct disease subtypes and correlates with high expression of EZH2. *Oncogene*. 2015;34:5869-78.
38. Donawho CK, Luo Y, Luo Y, Penning TD, Bauch JL, Bouska JJ, et al. ABT-888, an orally active poly(ADP-ribose) polymerase inhibitor that potentiates DNA-damaging agents in preclinical tumor models. *Clin Cancer Res*. 2007;13:2728-37.
39. Horton TM, Jenkins G, Pati D, Zhang L, Dolan ME, Ribes-Zamora A, et al. Poly(ADP-ribose) polymerase inhibitor ABT-888 potentiates the cytotoxic activity of temozolomide in leukemia cells: influence of mismatch repair status and O6-methylguanine-DNA methyltransferase activity. *Mol Cancer Ther*. 2009;8:2232-42.
40. Liu X, Shi Y, Guan R, Donawho C, Luo Y, Palma J, et al. Potentiation of temozolomide cytotoxicity by poly(ADP)ribose polymerase inhibitor ABT-888 requires a conversion of single-stranded DNA damages to double-stranded DNA breaks. *Mol Cancer Res*. 2008;6:1621-9.
41. Palma JP, Rodriguez LE, Bontcheva-Diaz VD, Bouska JJ, Bukofzer G, Colon-Lopez M, et al. The PARP inhibitor, ABT-888 potentiates temozolomide: correlation with drug levels and reduction in PARP activity in vivo. *Anticancer Res*. 2008;28:2625-35.
42. Tentori L, Ricci-Vitiani L, Muzi A, Ciccarone F, Pelacchi F, Calabrese R, et al. Pharmacological inhibition of poly(ADP-ribose) polymerase-1 modulates resistance of human glioblastoma stem cells to temozolomide. *BMC Cancer*. 2014;14:151.
43. Hegi ME, Diserens AC, Gorlia T, Hamou MF, de Tribolet N, Weller M, et al. MGMT gene silencing and benefit from temozolomide in glioblastoma. *N Engl J Med*. 2005;352:997-1003.
44. Tang SW, Bilke S, Cao L, Murai J, Sousa FG, Yamade M, et al. SLFN11 Is a Transcriptional Target of EWS-FLI1 and a Determinant of Drug Response in Ewing Sarcoma. *Clin Cancer Res*. 2015;21:4184-93.
45. Tian L, Song S, Liu X, Wang Y, Xu X, Hu Y, et al. Schlafen-11 sensitizes colorectal carcinoma cells to irinotecan. *Anticancer Drugs*. 2014;25:1175-81.
46. Willers H, Taghian AG, Luo CM, Treszezamsky A, Sgroi DC, Powell SN. Utility of DNA repair protein foci for the detection of putative BRCA1 pathway defects in breast cancer biopsies. *Mol Cancer Res*. 2009;7:1304-9.
47. Nogales V, Reinhold WC, Varma S, Martinez-Cardus A, Moutinho C, Moran S, et al. Epigenetic inactivation of the putative DNA/RNA helicase SLFN11 in human cancer confers resistance to platinum drugs. *Oncotarget*. 2016;7:3084-97.
48. Gardner EE, Lok BH, Schneeberger VE, de Stanchina E, Poirier JT, Rudin CM. Loss of SLFN11 or gain of TWIST1 promote chemotherapy resistance in small cell lung cancer [abstract]. In: Proceedings of the 107th Annual Meeting of the American Association for Cancer Research; 2016; New Orleans, LA: Philadelphia (PA): AACR; 2016. Abstract nr 4187.
49. Murai J, Zhang Y, Morris J, Ji J, Takeda S, Doroshow JH, et al. Rationale for poly(ADP-ribose) polymerase (PARP) inhibitors in combination therapy with camptothecins or temozolomide based on PARP trapping versus catalytic inhibition. *J Pharmacol Exp Ther*. 2014;349:408-16.
50. Smith MA, Reynolds CP, Kang MH, Kolb EA, Gorlick R, Carol H, et al. Synergistic activity of PARP inhibition by talazoparib (BMN 673) with temozolomide in pediatric cancer models in the pediatric preclinical testing program. *Clin Cancer Res*. 2015;21:819-32.

Figure Legends

Figure 1. PARP inhibitor sensitivity in SCLC correlates with *SLFN11* gene expression and varies based on PARP trapping potency. **(A)** Scatterplot of area under the curve IC₅₀ drug sensitivity data from the Genomics of Drug Sensitivity in Cancer (GDSC) available datasets of three different PARP inhibitors. R and p values from Spearman's rank correlation tests are displayed. **(B)** Volcano plot of the mean -ln IC₅₀ (μ M) of all three PARP inhibitors identified *SLFN11* as a highly significant gene by log odds with the large gene expression variation according to drug sensitivity (Supplemental Table 2). **(C)** SCLC cell lines with greater *SLFN11* gene expression are more sensitive to PARP inhibitors and standard cytotoxic chemotherapy. **(D)** SCLC cell lines are more sensitive to PARP inhibitors with greater PARP trapping potency. Veliparib, the least potent PARP trapper, and rucaparib exhibit greater IC₅₀ in SCLC as compared to all other tumor cell lines (* $p = 0.03$ for both drugs by Wilcoxon-Mann-Whitney test). Differences between the IC₅₀ of SCLC cell lines compared to all other tumor cell lines were not statistically significant by t-tests for olaparib.

Figure 2. SCLC cell line sensitivity to talazoparib depends on *SLFN11*. **(A)** Talazoparib sensitivity in SCLC cell lines was stereospecific and correlated with *SLFN11* gene and protein expression. A near infrared Western blot against the labeled proteins is displayed. **(B)** Linear regression of *SLFN11* protein levels normalized to actin as detected by near infrared Western blotting and talazoparib sensitivity demonstrated a strong correlative trend ($p = 0.06$) R and p values by Spearman's rank correlation test.

Figure 3. Loss of *SLFN11* confers resistance to PARP inhibition in SCLC. **(A)** *Left:* shRNA sequences against *SLFN11* and Renilla luciferase (REN) as a control were cloned into the LT3GEPIR doxycycline inducible vector. DMS114 cells stably expressing these constructs were subjected to vehicle or doxycycline at 1 μ g/mL or 2 μ g/mL concentrations for 48h. Western blotting by near infrared is displayed. *Right:* Cells were exposed to 1 μ g/mL of doxycycline for 48h prior to plating and were then treated with a range of talazoparib doses 24h after plating. After 5d of drug exposure, a resazurin conversion assay was performed. Data represent the mean \pm SD of 3 replicates. **(B)** *Left:* sgRNA sequences against *SLFN11* were cloned into a lentiCRISPR v2 backbone and transduced into NCI-H526 cells to generate stable *SLFN11*-knockout(KO) lines. Western blot by chemoluminescence is shown. *Right:* A resazurin conversion assay of the labeled stable cell lines were performed after 5d of exposure to a range of talazoparib doses. Data represent the mean \pm SD of 3 replicates.

Figure 4. SLFN11 protein expression correlates with talazoparib efficacy in patient-derived xenografts and *SLFN11* mRNA is expressed bimodally in primary patient samples. **(A)** Representative images of immunohistochemical staining against SLFN11 for all tested PDXs are shown. The H-score and modified H-score (H_{mod}) for SLFN11 nuclear staining for each PDX model is displayed. Scale bar, 50 μ m. **(B)** Percent change in tumor volume at end of study for each individual animal and displayed in order of SLFN11 H-score. End of study difference in tumor size between vehicle and treatment groups were significant for JHU-LX22, JHU-LX110, and SCRXLu149 ($p = 0.0286$, $p = 0.0286$, $p = 0.0079$, respectively) P -values by the Wilcoxon-Mann-Whitney test. **(C)** Percent tumor growth inhibition for each PDX model. Mean \pm SD shown. The delta method was used to compute the variance used for SD calculations. **(D)** *SLFN11* gene expression of primary SCLC samples plotted with publically available datasets from The Cancer Genome Atlas (TCGA) of other histologies are displayed here. The inset displays a bimodal distribution of *SLFN11* gene expression (*blue dashed line*). Median \pm SD shown.

Figure 5. Talazoparib is synergistic with temozolomide *in vitro*. **(A)** *Left:* Drug synergy matrix of talazoparib and TMZ in the NCI-H146 cell line is shown. A resazurin conversion assay was performed after 5d of drug treatment. *Right:* Excess over highest single agent (HSA) response is displayed showing the range of excess response in the 1 : 70 to 1 : 700,000 ratio range of talazoparib : TMZ. **(B)** Near infrared Western blot against MGMT in the indicated cell lines. **(C)** Median effect plot of a MGMT low (NCI-H146) and high (NCI-H82) cell lines. A resazurin conversion assay was performed after 5d of drug treatment. Fa, fraction affected and Fu, fraction unaffected. **(D)** Combination indices of MGMT high and MGMT low labeled cell lines are displayed. Two-fold serial dilutions of the combination drug are displayed. The 0.002 : 20 (μ M) dose of talazoparib : TMZ is highlighted in purple.

Figure 6. Talazoparib and temozolomide exhibit marked combinatorial efficacy in patient-derived xenografts. **(A)** Western blot against MGMT by near infrared imaging in PDX models. **(B)** Tumor volume growth curves of 7 PDX models treated with the labeled single drug or combination. $n = 4-5$ per arm. Mean tumor volume \pm SD shown.

Figure 1

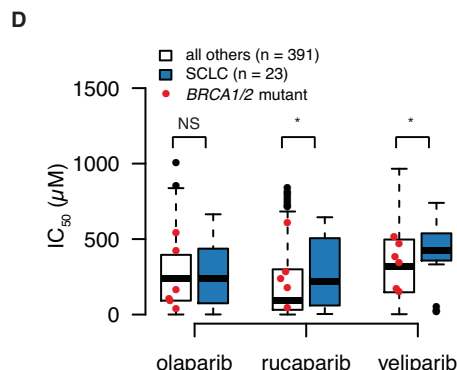
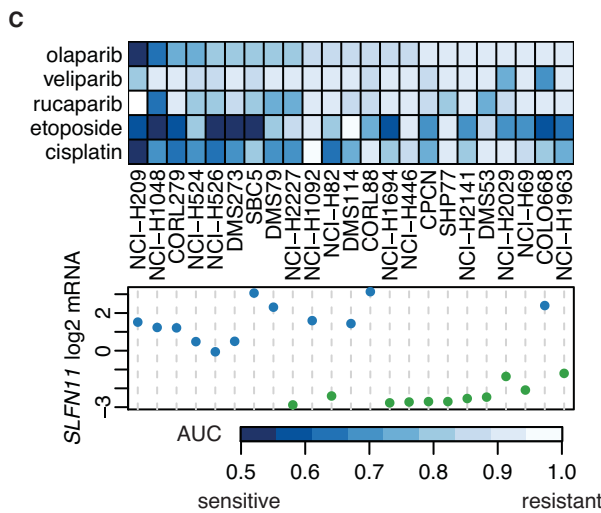
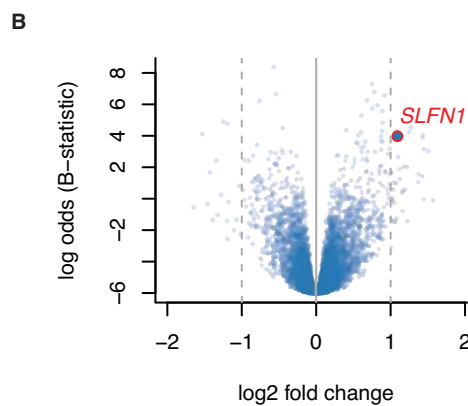
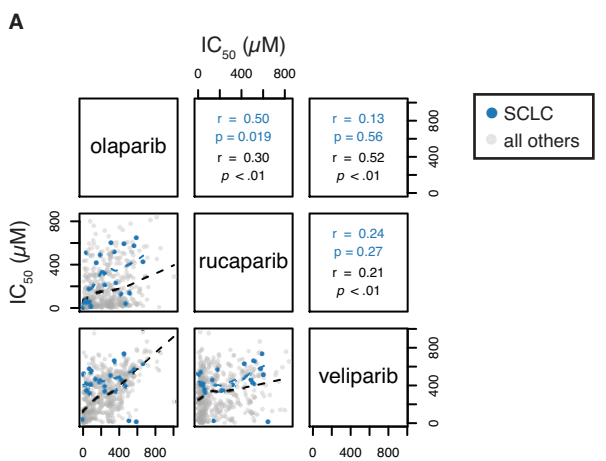


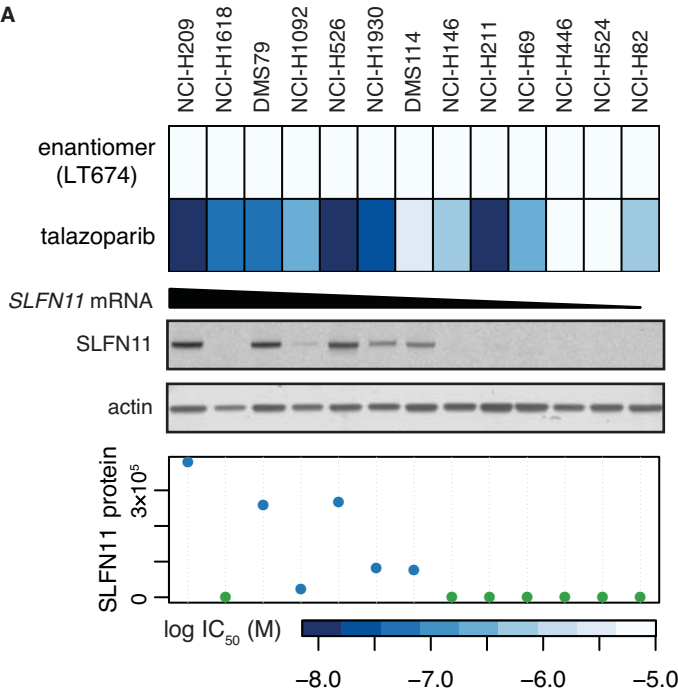
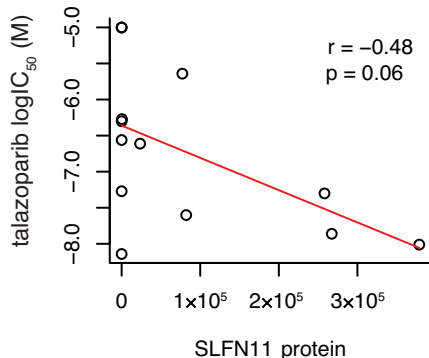
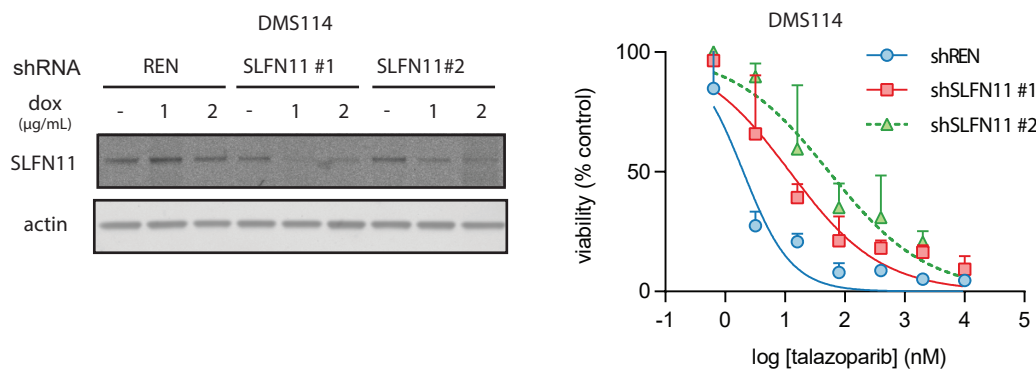
Figure 2**A****B**

Figure 3

A



B

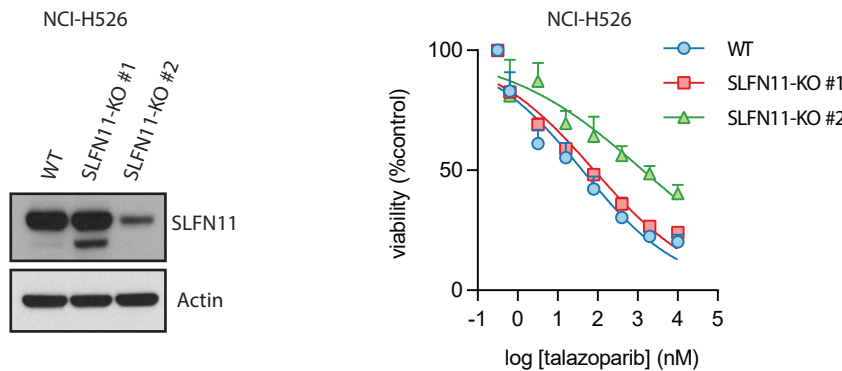
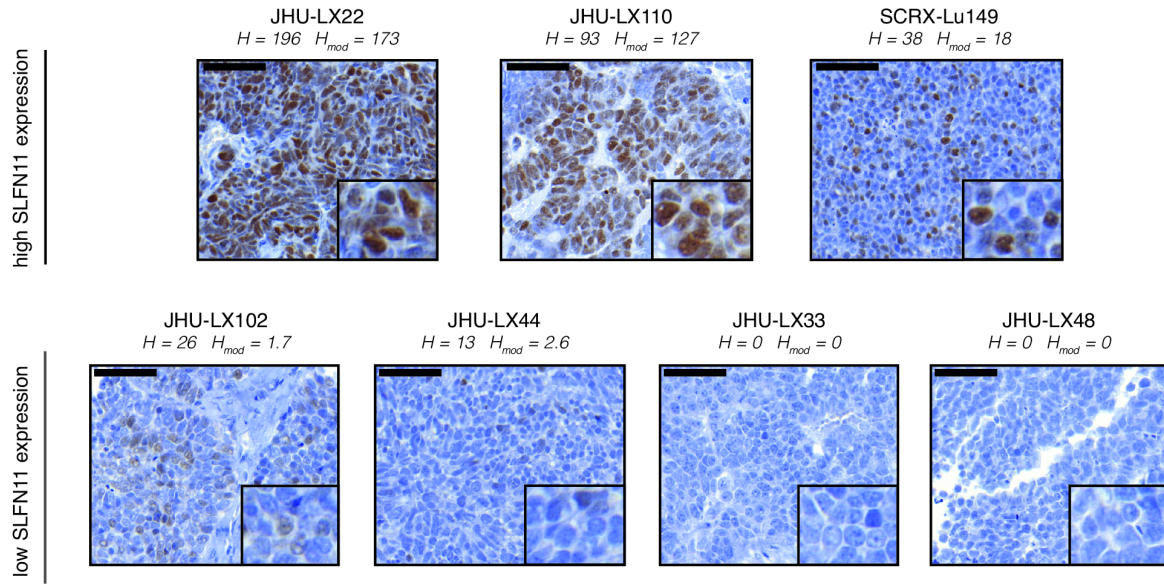
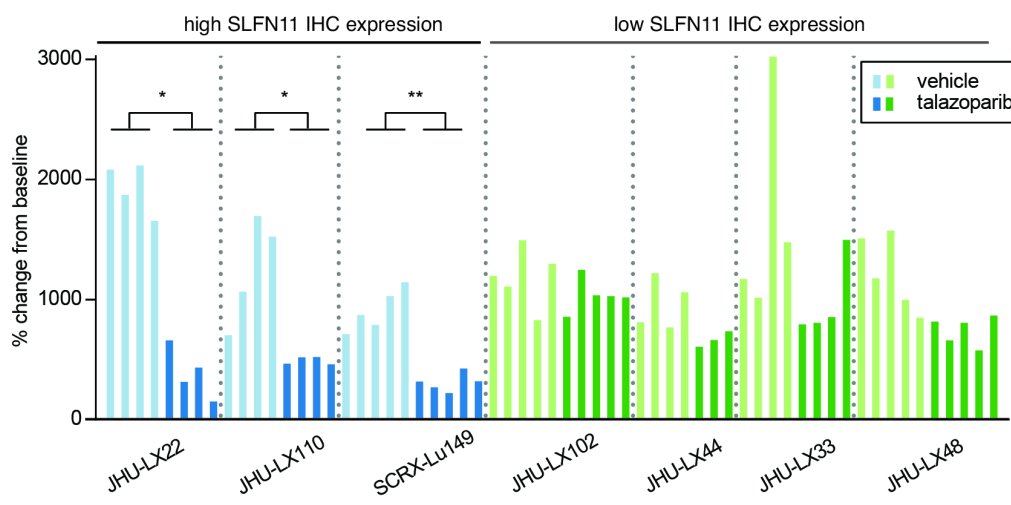


Figure 4

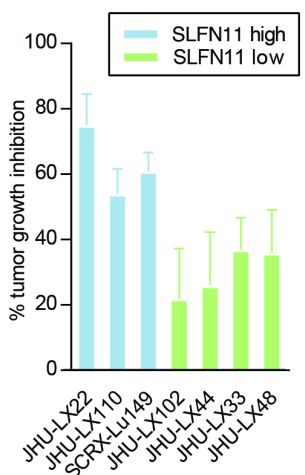
A



B



C



D

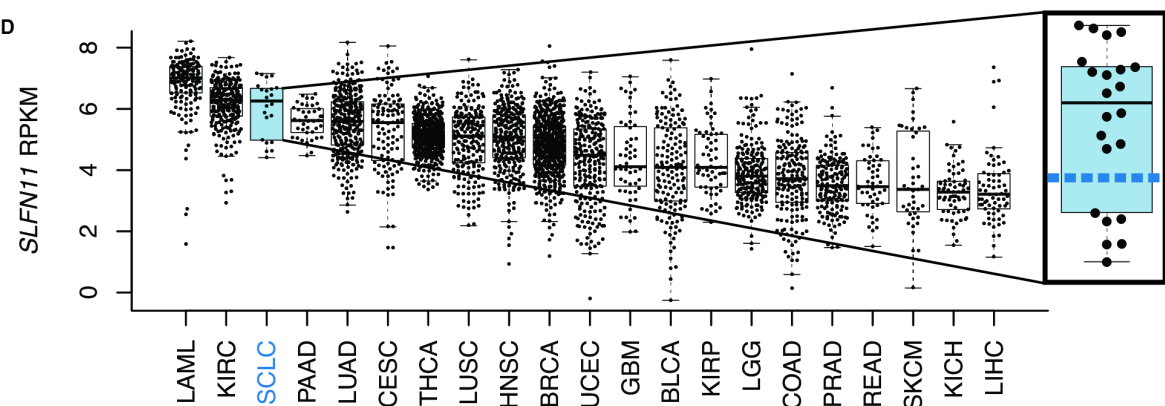


Figure 5

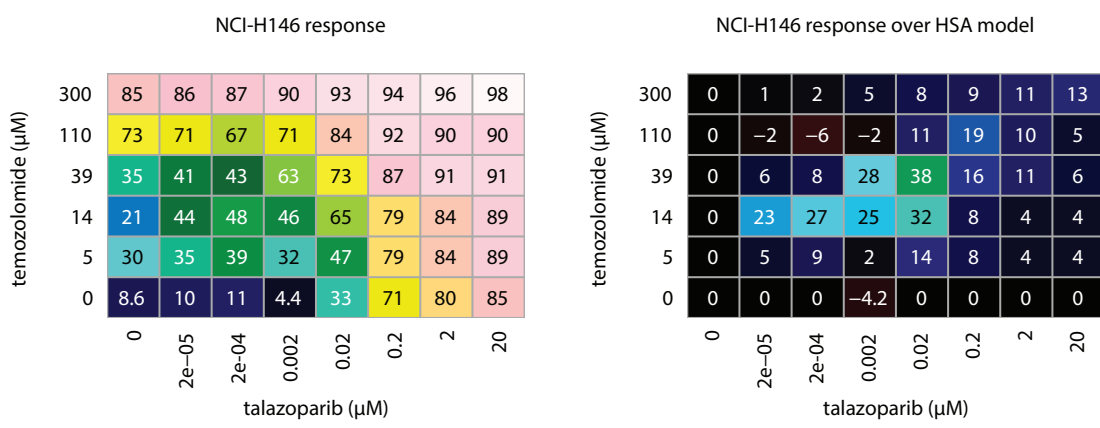
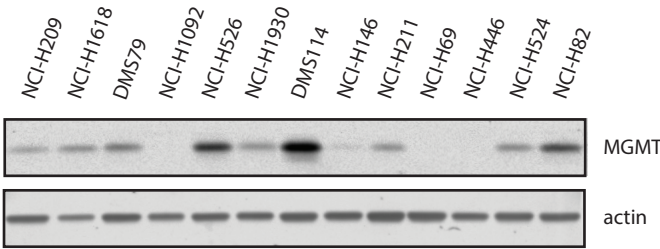
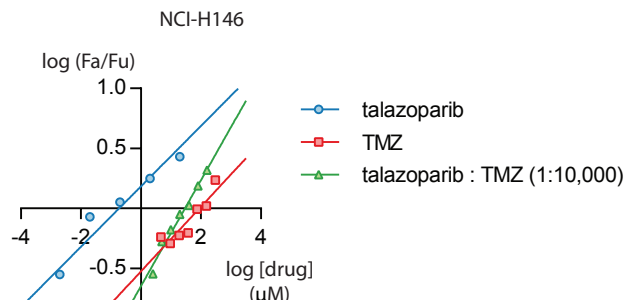
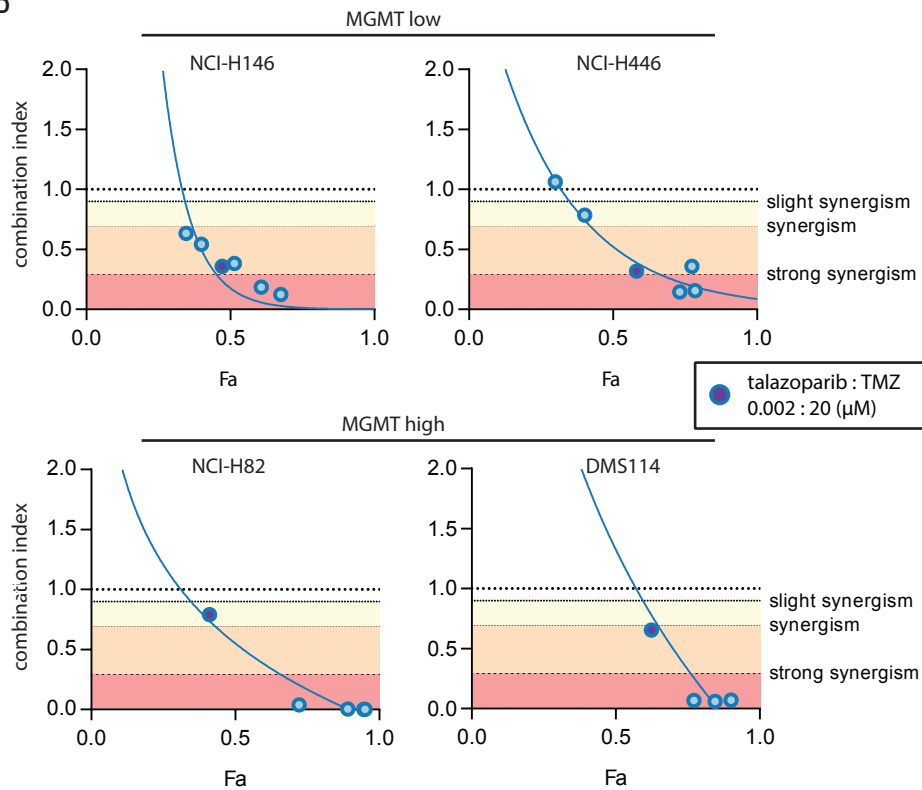
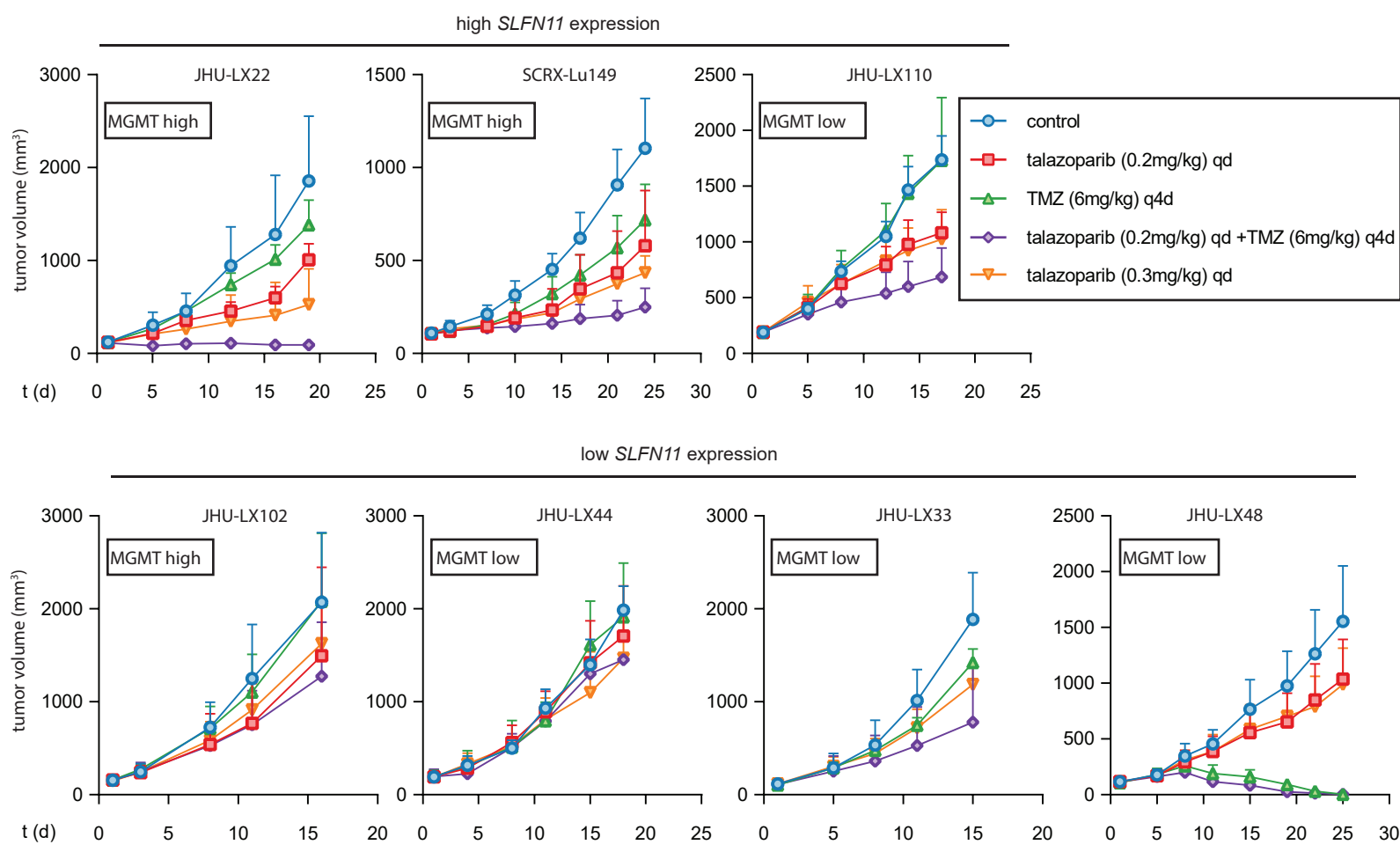
A**B****C****D**

Figure 6

A



B

